OPTIMIZATION OF THE RECONSTRUCTION PARAMETERS IN COMPUTER GENERATED HOLOGRAMS AND DIGITAL HOLOGRAPHY

Mona MIHĂILESCU[1], Alexandru M. PREDA[2], A. SOBETKII[3], Eugen I. SCARLAT[4], Liliana PREDA[5]

Lucrarea prezintă un algoritm bazat pe folosirea transformatei Fourier rapide, folosit atat la refacerea fazei in hologramele generate pe computer (CGH), cat si pentru reconstructia numerica in holografia digitala (DH), impunand diferite seturi de constrangeri in planul de intrare si in planul de iesire. Influenta fazei initiale, ca parametru in proiectarea CGH, este prezentata prin evolutia abaterii patratice medii, a eficientei difractiei, si a contrastului in spoturile dorite. Pornind de la matricea obtinuta cu parametrii optimizati ai CGH, au fost realizate elemente optice difractive (DOE) in sticla, iar imaginile obtinute au fost analizate experimental. In DH se porneste de la un obiect real a carui holograma este inregistrata pe CCD, iar reconstructia este facuta numeric. Influenta conditiilor experimentale (intensitatea radiatiei laser, distanta dintre sursa punctiforma si obiect) in imaginea obiectului reconstruit este, de asemenea, prezentata.

The phase retrieval algorithm based on the fast Fourier transform was used either to design computer generated hologram (CGH) or for numerically reconstruction of the object starting from the experimental holograms recorded on the CCD in digital holography (DH) subjected to different sets of constraints in the input and output planes. The influence of the initial phase, acting as a command parameter in CGH design, is presented in terms of the mean square error, diffraction efficiency, and contrast in the desired spots. The ideal CGH obtained is imprinted on a glass and its image is then physically reconstructed. Different parameters of the experimentally image are presented. The influence of the experimental conditions (intensity of the laser radiation and the distance between the source and the object) in the digital in-line hologram and its reconstruction is also presented.

Keywords: digital holography, numerical reconstruction, computer generated holograms, diffractive optical elements.

[1] Assist., Physics Departament, University "Politehnica" of Bucharest, ROMANIA
[2] Prof., Physics Departament, University "Politehnica" of Bucharest, ROMANIA
[3] Researcher, S. C. OPTICOAT S.R.L., Bucharest, ROMANIA
[4] Lecturer, Physics Departament, University "Politehnica" of Bucharest, ROMANIA
[5] Lecturer, Physics Departament, University "Politehnica" of Bucharest, ROMANIA

1. Introduction

Based on the Gabor's holographic principles, nowaday a lot of optical phenomena and techniques are developed. Modern holography includes a) the design of DOEs as a special case of CGHs applied for beam shaping, splitting and steering [1], optical interconnections [2], optical tweezers [3], multiphoton spectroscopy [4], lithographic fabrication of photonic crystals [5], and b) DH like a useful method for non-destructive testing in: object contouring [6], biological microscopy [7], measurement of moving objects [8], characterization of micro-optical components [9], systems with CD and DVD [10], in X-ray microscopy [11]. When the wavefront is recorded on arbitrary surfaces, we can solve the so called "inverse problem" and to understand the tomographic imaging technique [12].

For CGH, we started with a given (numerically) intensity distribution acting as a virtual object in the output plane aiming to find out the phase in the input plane [13], which is then converted into a physical phase-only DOE fabricated via the e-beam and reactive ion etching procedures. Then, depending on the design of the experimental arrangement, the incident laser beam forms in the far field or in the near field the corresponding real diffractive pattern of the initial virtual object.

In DH, we started with a real object. Its in-line hologram is succesively recorded on the CCD, discretized, filtered, and stored in the computer as data files; no chemical process is needed and the time is shorter than in a classical holography. The last part – calculation of the phase and amplitude distribution of the reconstructed real object in the output plane, is done by using the well-known diffraction integral [14].

In both the above mentioned numerical techniques, an iterative process based on the Gerchberg-Saxton [15] algorithm is used [16, 17], with different set of constraints in the input and output planes. At every iteration, we calculate the difference between the desired image and the current one in the terms of the mean square error [13], diffraction efficiency, and contrast. The influence of the initial phase in the design of CGH is analyzed with respect to the convergence of the process. The resulted ideal CGH is fabricated in glass and the image is then physically reconstructed. Different parameters of the experimental image are presented in section 3.

In the digital in-line holography (DIH), the CCD records the superposition of the reference wavefront and the object one. The experimental conditions (intensity of the laser radiation, the distance between the source and the object, etc.) does influence the recorded image and also the numerical reconstruction. The analysis is presented in section 3.

2. Theory

Let us consider the diffraction of monochromatic, unit amplitude, plane wave, normally impinging on an aperture in the input plane (the hologram plane) characterized by the complex transmission function: $t(x,y) = a(x,y)\exp(i\varphi(x,y))$. Thus, the complex wave field in the output plane $W(\tilde{x},\tilde{y}) = A(\tilde{x},\tilde{y})\exp(i\psi(\tilde{x},\tilde{y}))$ at the distance z from input plane, can be described by the Rayleigh-Sommerfeld integral [14]:

$$W(\tilde{x},\tilde{y}) = \iint_{\Sigma} t(x,y)S(x,y,\tilde{x},\tilde{y})dxdy\,, \tag{1}$$

where

$$S(x,y,\tilde{x},\tilde{y}) = \frac{\exp(ikr)}{i\lambda z} \tag{2}$$

is the point spread function, which gives us information about the spatial extent in the output plane.

In the Fresnel's approximation (when $z^3 >> \frac{\pi}{4\lambda}\left[(x-\tilde{x})^2 + (y-\tilde{y})^2\right]^2$), Eq. (2) becomes:

$$S_n(x,y,\tilde{x},\tilde{y}) = \frac{\exp(i\lambda z)}{ikz}\exp\left\{\frac{ik}{2z}\left[(x-\tilde{x})^2 + (y-\tilde{y})^2\right]\right\}, \tag{3}$$

and then the complex field from Eq.(1) looks like the convolution between the transmission function of the aperture and the point spread function:

$$W(\tilde{x},\tilde{y}) = t(x,y) \otimes S_n(x,y,\tilde{x},\tilde{y}) = G_{Fr}(t)\,, \tag{4}$$

Where the symbol $\otimes$ means the mathematical operation of convolution. It can be reformulated using the convolution theorem and implemented in MATLAB with the fast Fourier transform (FFT).

In the Fraunhofer's approximation (satisfied if $z >> \frac{k(x^2+y^2)}{2}$), Eq.(1) becomes:

$$W(\tilde{x},\tilde{y}) = \frac{\exp(ikz)}{i\lambda z}\exp\left[\frac{ik}{2z}(\tilde{x}^2 + \tilde{y}^2)\right]FFT(t(x,y)) = G_{Fo}(t)\,, \tag{5}$$

where λ is the wavelength of the incident radiation, $k = 2\pi/\lambda$ is the wavenumber, (x,y) are the coordinates in the hologram plane (input plane), $(\tilde{x},\tilde{y})$ are the coordinates in the image plane (output plane), r is the distance between any point between the input plane and the image plane, FFT is the fast Fourier transform, G_{Fr} expresses the Fresnel transformation operator, while G_{Fo} is the symbol of the overall Fourier operator that changes the variables (*x,y*) into the spatial frequencies $p = \tilde{x}/z\lambda$, $q = \tilde{y}/z\lambda$. A generalization of the Eqs.(4) and (5) can be written:

$$W(\tilde{x},\tilde{y}) = G\big(t(x,y)\big), \tag{6}$$

where G is an operator meaning either the Fresnel or Fourier operator.

We work in MATLAB with discrete functions and transforms by sampling the continuous one and taking care on the under-sampling [18]. The discrete pixel sizes in the input plane Δx and Δy are related with the sizes of the pixels in the output plane, $\Delta\tilde{x}$ and $\Delta\tilde{y}$, by the following relation [19]:

$$N\Delta x\Delta\tilde{x} = \lambda z \quad \text{and} \quad M\Delta y\Delta\tilde{y} = \lambda z\,, \tag{7}$$

where N and M are the pixel number in the output plane along the axes. The reconstructed wave field is the solution of the Eqs.(4) and (5), is a good approximation of the object provided that the Nyquest theorem is fulfilled.

A flowchart of the processes involved in CGH and DH is presented in Fig. 1. In both processes, we have one step experimental and one step digital, but the succession is reversed: 1) the first step – hologram generation – is digital in CGH (virtual object) and experimental in DH (real object), 2) the second step – reconstruction – is experimental in CGH and digital in DH.

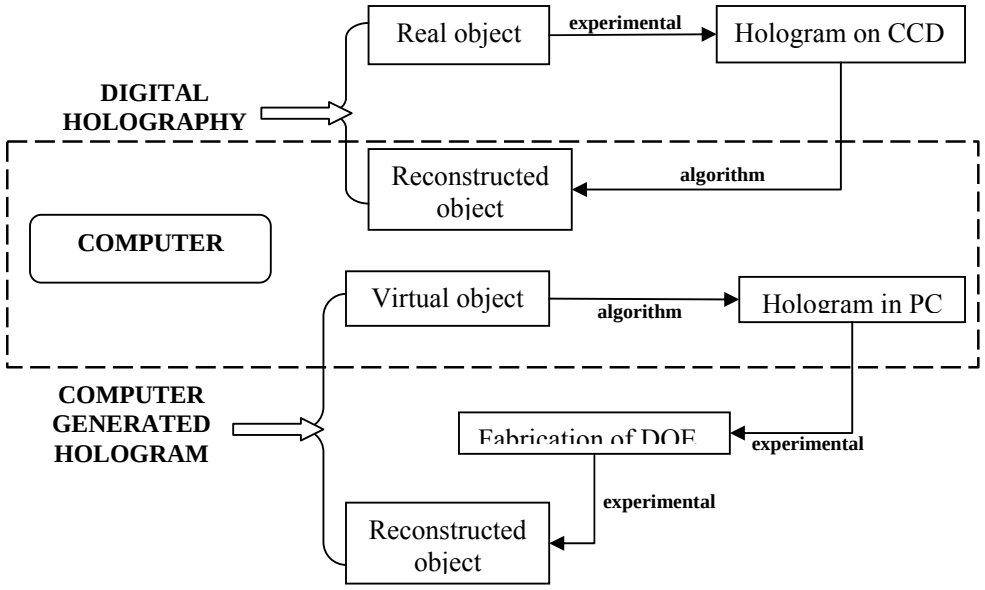

Fig. 1 A flowchart with the processes involved in CGH and DH

3. Simulations and experimental setup

In Fig. 2 we present a flow chart of the Gerchberg-Saxton [15] algorithm implemented in MATLAB and used in CGH and DH, but with different sets of constraints in the input plane (hologram plane) and the output plane (object

plane). In CGH the constraints are *i)* in the hologram plane: discretized phase and constant unit amplitude for the phase only DOE, and *ii)* in object plane: amplitude equal with the one of the virtual object. Conversely, in DH we impose the constraints *i)* in the hologram plane: amplitude equal with the recorded one, and *ii)* in object plane: imaginary part equal with zero for real object, or amplitude constant equal with unity for phase only objects, or phase constant equal with zero for amplitude only objects.

In the case of the CGH design, we started the algorithm with a desired image file in the output plane (desired spots in the signal window surrounded by zero elements). In the case of the reconstructed object in DH, the algorithm is started with the CCD hologram as an image file in the input plane. For the CGH design, the operator *G* was used in the Fraunhofer approximation; for DH design, the operator *G* was used in the Fresnel approximation.

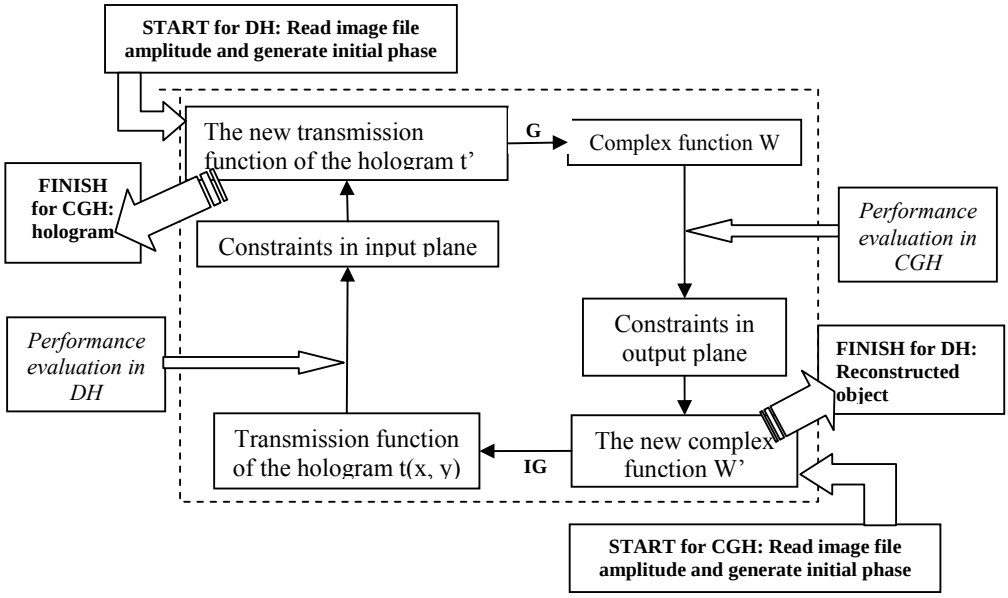

Fig. 2 The block diagram of the algorithm (surrounded by dashed line) and specific parts for CGH and DH

At every iteration, performance is evaluated by calculating the parameters which give us information about the quality of the numerically generated image as well as about the convergence rate of the algorithm, i.e.:

1) The mean square error [13]: *MSE* as the difference between the calculated intensity and desired one from initial image file

2) The diffraction efficiency: η as the ratio between the intensity in the signal window and the whole diffracted intensity.

3) The contrast in a given image: $C = \frac{Intens_{\max} - Intens_{\min}}{Intens_{\max} + Intens_{\min}}$, where $Intens_{\max}$ and $Intens_{\min}$ are the maxim and minimum values from all pixels of the intensity image, respectively.

If the values for the *MSE* and *C* are under the desired threshold, the algorithm will be stopped; the CGH and reconstructed object in DH will be the last files obtained with these names.

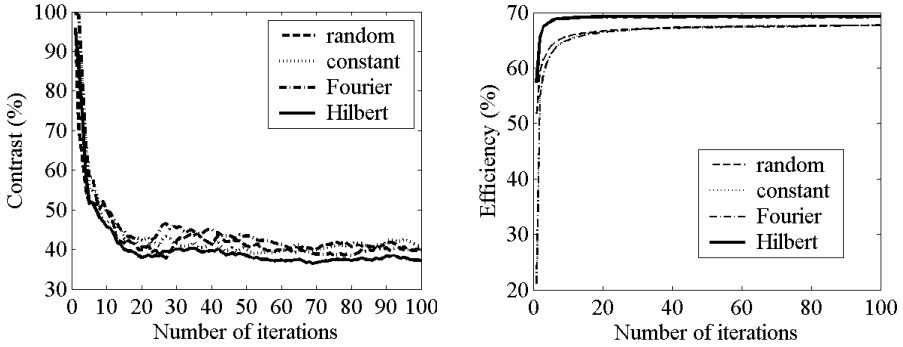

Fig. 3 a) The contrast inside the desired spots; b) The diffraction efficiency when the initial phase in output plane is generated: random, constant, with Fourier transform, with Hilbert transform

In the CGH design, we have studied a lot of parameters [20] like as the number of phase levels, the gray levels surrounding the desired spots in the signal window, the number of the step where we put the constraints for the discretized phase. Now we discuss the initial phase associated with the desired image in signal window, which can be random, constant, or generated with Fourier transform or Hilbert transform associated with the initial image, like in the image processing [21]. In Fig. 3 we present the diffraction efficiency and the contrast for CGH designed in these four cases. We observe that the best value for parameters are obtained when the initial phase is generated with Hilbert transform associated with the desired object.

The last matrix obtained in MATLAB (i.e. at the end of the algorithm) for CGH (fig. 4b), was used for the DOE fabrication. Two wafers were used: W1 = borosilicate glass (3±0.5mm thick) covered with Cr (500nm thick) and electronoresist and W2 = BK7 glass with thin film Cr+CrO_2 deposition. On W1 we fabricated the mask and on W2 we fabricated the DOE. The steps in technological process are: (1) mask fabrication with e-beam on W1, (2)

electronoresist removal, (3) surface control, (4) photoresist spin coated on W2, (5) mask transfer on W2 through reactive ion etching, (6) chemical etching of $Cr+CrO_2$, (7) photoresist removal, (8) surface control. Then, we put the fabricated DOE (Fig. 4c) in the laser beam, and it gives us the reconstructed object (Fig. 4d) in good agreement with the initial one from the signal window (Fig 4a). The resolution in mask fabrication was 1μm/pixel.

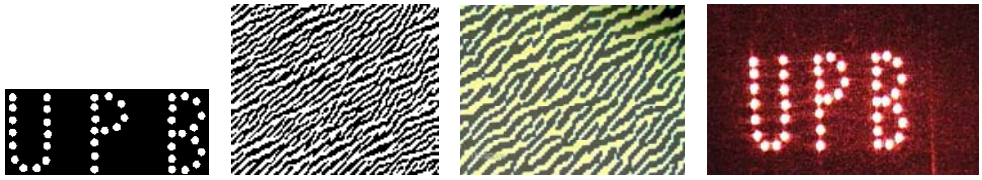

a) b) c) d)

Fig. 4 a) The signal window in the initial image file for CGH in output plane; b) The last image file obtained from algorithm – the hologram in CGH; c) The fabricated structure of DOE from CGH; d) experimentally reconstruction from object from image a).

The first step in digital in-line holography (DIH) is experimentally. We use an experimental setup (Fig. 5) with laser (HeNe 632.8nm), pinhole (10μm), different objects with maximum dimension – a – which satisfies the condition: $a^2 << z\lambda$ and a CCD (Sony, DCR-TRV140E).

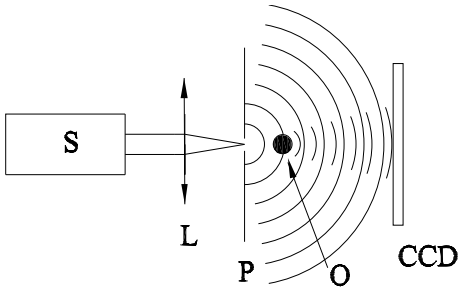

Fig. 5 The experimental setup for DIH: S –HeNe laser; L – lens; P – pinhole; O – object.

Digital holograms (Fig.6a) recorded on the 576×768 pixels CCD image, are transmitted to a computer and are encoded in 256 gray levels in an indexed image file to be read in MATLAB. There we subtracted the background and filter the image with wavelet function [22] (Fig. 6b). In order to have some information about the dimension of one pixel in the reconstructed image (Fig. 6c) in MATLAB, we used three different wires (with diameters of 66μm, 25μm and 14μm) and we calibrate our experimental setup.

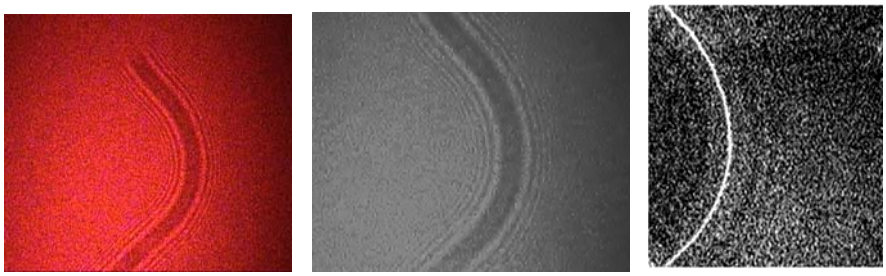

a) b) c)

Fig. 6 a) The hologram; b) the filtered hologram; c) the reconstructed image

Numerical reconstruction in DIH is influenced by the quality of the hologram recorded on CCD, which depends by several experimental factors: (1) wavelength; (2) distance between pinhole and object, (3) pinhole diameter d, which controls spatial coherence and illumination cone; (4) numerical aperture $NA = \frac{L}{2}\sqrt{\left(\frac{L}{2}\right)^2 + D^2}$, depending by the width L of the CCD and distance D between pinhole and CCD [23]; (5) pixel density and size in the CCD sensor; (6) intensity of the laser radiation in the contrast and the brightness of the recorded and reconstructed images.

4. Results

We recorded on a CCD the image for many reconstructed objects in CGH with different size for the signal window, and different number of pixels for each spots in signal windows; the results for diffraction efficiency and contrast for these experimentally images are given in tables 1 and 2.

Table 1

The size of the signal window (pixels x pixels)	76 x 76	96 x 208	310 x 110	150 x 530	168 x 550
The diffraction efficiency (%)	55.8	57.3	58.1	61.8	62.3

Table 2

The size of the desired spots (pixels x pixels)	2 x 2	4 x 4	6 x 6	8 x 8
The contrast in the desired spots (%)	1.23	3.15	6.57	9.26

In order to study the influence of the intensity of the incident laser radiation upon the recorded hologram, and therefore upon reconstructed object, we use a neutral optical density filter and we choose 11 steps on it, while the real

object is one wire with 66μm diameter. The recorded holograms are differring each other by the contrast and brightness [21]: small value for contrast when the intensity is small (Fig. 7a), but also when it is big. The contrast and brightness in the interesting region in the reconstructed image (obtained with the algorithm presented in the previous section – in the Fresnel approximation) are given in Fig. 8b). In Fig. 8a) we plot several cross-sections for different reconstructed images (in interest region) recorded at different incident intensities ($I_1<I_2<I_3<I_4$ – the first four steps).

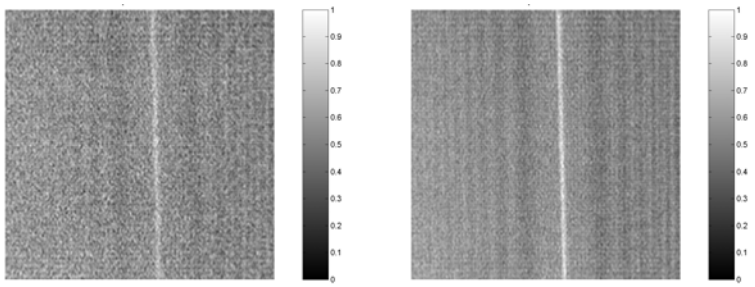

a) b)

Fig. 7 The reconstructed amplitude when the hologram is recorded with the intensity in first step a); and fourth step b).

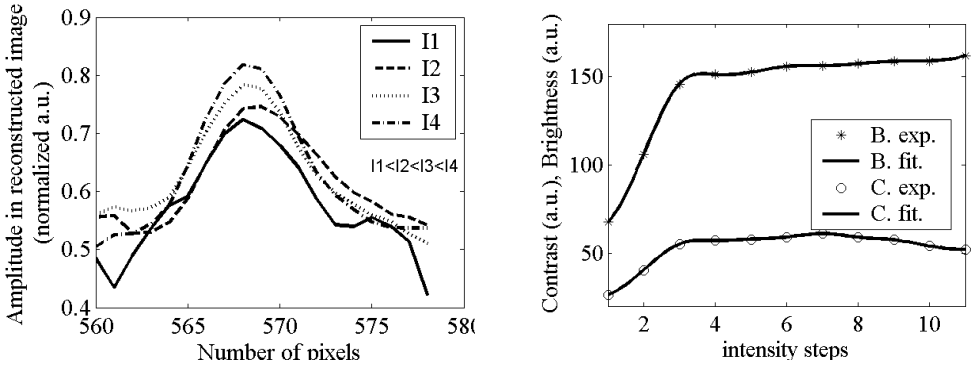

Fig. 8 a) A cross section from reconstructed amplitude from holograms recorded at different laser intensity; b) The contrast and brightness in reconstructed amplitude from holograms recorded at different laser intensity

The distance between the pinhole and the object (a simple wire with the diameter of 25μm), also influences the quality of reconstructed image through the size of the fringes in the hologram plane. The smallest size of the fringes has to be greater than the dimension of one pixel, otherwise the information contained into that domain is lost. Also, the size of the whole diffractive pattern must be smaller than the width L of the CCD. We can work only with the distances in the interval

3-5cm with a step of 1mm. In this interval, the maximum values in the reconstructed amplitude decreases when increasing the distance (Fig. 9b). In Fig. 9a) we plot several sections for different reconstructed images (in the analyzed region) that were recorded at different distances between pinhole and the object ($d_1<d_2<d_3<d_4$). The displacement of the maxima along the x direction is because of the instability of our mechanical devices, but it did not exceed 3 pixels.

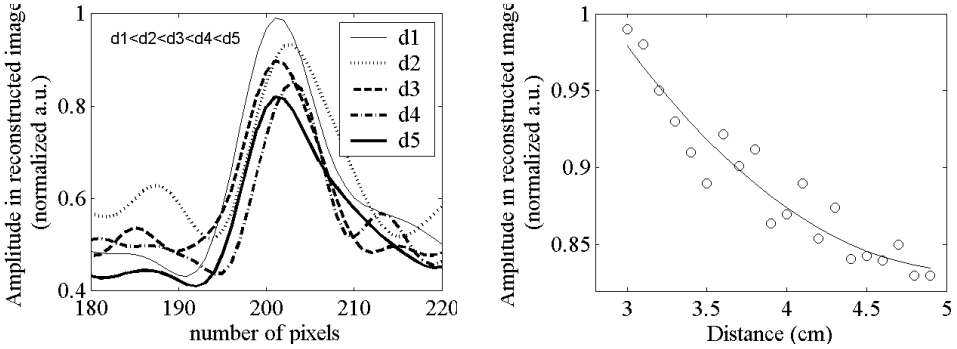

Fig. 9 a) A cross section from reconstructed amplitude from holograms recorded at different distances pinhole-object; b) The maximum value in reconstructed amplitude from holograms recorded at different distances pinhole-object

5. Discussions and conclusions

In the CGH design for DOE fabrication, we had four different initial phase in the output plane: random phase, constant phase, Fourier generated, and Hilbert generated, like in the image processing. After 100 iterations of the algorithm, the values for the diffraction efficiency differ with no more than 0.01% whichever the case. The contrast also had near values.

The digital reconstruction process involved in DIH makes it a tool for obtaining rapidly from a single hologram a wide range of information. The intensity of the incident laser radiation is important in the DIH reconstruction. When the contrast between fringes is small, the reconstructed amplitude in output plane has a small value. We obtained bigger values for the amplitude of the reconstructed object, when the intensity began to saturate with respect to the CCD.

At small distances between the pinhole and the object, the size of the fringe was big, but one has to be careful at the numerical aperture of the CCD, because there exists the danger to record only a part of the hologram. When removing the object from the pinhole, the size of the fringes became smaller and

smaller and also the reconstructed amplitude. The limit is one fringe on two pixels of the CCD, according to the Whittaker-Shannon sampling theorem.

REFERENCES

[1] *G. Mínguez-Vega, E. Tajahuerce, M. Fernández-Alonso, V. Climent, J. Lanci, J. Caraquitena, P. Andrés,* Dispersion-compensated beam-splitting of femtosecond light pulses: Wave optics analysis, Opt. Express, 15, 2007, 278-288

[2] *J. Liu, M. Thomson, A. J. Waddie, M. R. Taghizadeh,* Design of diffractive optical elements for high-power laser applications, Opt. Eng. 43, 2004, 2541-2548

[3] *V. Emiliani, D. Cojoc, E. Ferrari, V. Garbin, C. Durieux, M. Coppey-Moisan, and E. Di Fabrizio,* "Wave front engineering for microscopy of living cells," Opt. Express 13,2005, 1395-1405

[4] *J. E. Jureller, H. Y. Kim, and N. F. Scherer,* Stochastic scanning multiphoton multifocal microscopy, Opt. Express 14, 2006, 3406-3414

[5] *X. L. Yang, L. Z. Cai, Y. R. Wang, and Q. Liu,* Interference of four umbrellalike beams by a diffractive beam splitter for fabrication of two-dimensional square and trigonal lattices , Opt. Lett. 28, 2003, 453-455

[6] *P. Ferraro, S. Grilli, D. Alfieri, S. De Nicola, A. Finizio, G. Pierattini, B. Javidi, G. Coppola, V. Strian,o* Extended focused image in microscopy by digital holography, Opt. Express 13, 2005, 6738-6750

[7] *C. J. Mann, L. Yu, M. K Kim,* Movies of cellular and sub-cellular motion by digital holographic microscopy Biomed Eng Online. 23, 2006, 5-21.

[8] *S. Satake, H. Kanamori, T. Kunugi, K. Sato, T. Ito, K. Yamamoto,* Parallel computing of a digital hologram and particle searching for microdigital-holographic particle-tracking velocimetr, Appl. Opt., 46, 2007, 538-550

[10] *F. Charrière, J. Kühn, T. Colomb, F. Montfort, E. Cuche, Y. Emery, K. Weible, P. Marquet, C. Depeursinge,* Characterization of microlenses by digital holographic microscopy, Appl. Opt., 45, 2006, 829-837

[11] *H. Horimai, X. Tan,* Collinear technology for a holographic versatile disk, Appl. Opt., 45, 2006, 910-922

[12] *Y. Zhang, X. Zhang,* Reconstruction of a complex object from two in-line holograms, Opt. Express, 11, 2003, 572-583

[12] *A. W. Lohmann, M. E. Testorf, J. Ojeda-Castaneda,* The Art and Science of Holography, H. J. Caulfield ed., SPIE Press, cap. 8, 2004

[13] *D. C. O'Shea, T. J. Suleski, A. D. Kathman, D. W. Prather,* Diffractive Optics – Design, Fabrication, and Test, Spie Press, Bellingham, Washington, USA, 2004,

[14] *J. W Goodman,* Introduction to Fourier optics, Mc Graw-Hill Book Company, 1968

[15] *R. W. Gerchberg and W. O. Saxton,* A practical algorithm of the determination of the phase from image and diffraction plane pictures, Optik 35, 1972, p. 237-246

[16] *A. Hermerschmidtd, S. Krüger, G. Wernicke,* Binary diffractive beam splitters with arbitrary diffraction angles, OPTICS LETTERS / Vol. 32, No. 5, 2007,448-450

[17] *Y. Zhang, G. Pedrini ,W. Osten, H. J. Tiziani,* Reconstruction of In-Line Holograms Using Phase Retrieval Algorithms, Physica Scripta. Vol. T118, 2005, 102–106

[18] *F. Nicolas, S. Coëtmellec, M. Brunel, D. Lebrun,* Suppression of the Moiré effect in subpicosecond digital in-line holography, Opt. Express, 15, 2007, 887-895

[19] *J. Garcia, D. Mas, R. G. Dorsch,* "Fractional-Fourier-transform calculation through the fast-Fourier-transform algorithm", Appl. Opt. 35 (1996) 7013
[20] *M. Mihailescu, L. Preda, Al. M. Preda, E. I. Scarlat,* "Modified Gerchberg-Saxton algorithm for diffractive optical element image retrieval", U. P. B. Sci. Bull., Series A, 674, 2005, 65-76
[21] *A. R. Weeks, Jr.,* Fundamentals of Electronic Image Processing, SPIE Opt. Eng. Press, third edition, 2004
[22] *A. Souvorov, T. Ishikawa, A. Kuyumchyan,* Multiresolution phase retrieval in the Fresnel region by use of wavelet transform JOSA A, 23, 2006, 279-287
[23] *J. Garcia-Sucerquia, W. Xu, S. K. Jericho, P. Klages, M. H. Jericho, H. Jürgen Kreuzer* Digital in-line holographic microscopy, Appl. Opt., 45, 2006, 836-848